

# Stable Metal-Organic Framework Based Electrode For Electrochemical Applications

Shi Wun Tong, Darren Chi Jin Neo, Wei Peng Goh, Changyun Jiang

*Institute of Materials Research and Engineering*

*Agency for Science, Technology, and Research (A\*STAR)*

Singapore

[tongsw@imre.a-star.edu.sg](mailto:tongsw@imre.a-star.edu.sg) (S. W. Tong) and [jiangc@imre.a-star.edu.sg](mailto:jiangc@imre.a-star.edu.sg) (C. Jiang)

**Abstract**—By electrodepositing a layer of Prussian blue (PB) on indium-tin-oxide substrate, followed by subsequent polyaniline (PANI) deposition, a bilayer PANI/PB electrode with high charge density ( $\sim 10 \text{ mC/cm}^2$ ) can be retained after 60 charging/discharging cycles. Compared with standalone PB electrode, the improvement in electrochemical properties and good morphological control were demonstrated based on PANI/PB electrode by using cyclic voltammetry and microscopic images respectively. This work paves a promising approach to prepare stable PB-based electrode for electrochemical devices.

**Keywords**—Metal-organic framework, Prussian blue, polyaniline, cyclic stability, electrodeposition, electrochromic

## I. INTRODUCTION

Prussian blue (PB)-a porous metal - organic framework has rendered its development in electrochromic (EC) devices, sensors, batteries and capacitors due to its unique electrochromic and electrocatalytic properties [1-6]. For EC devices, the presence of large interstitial voids and 3D ion diffusion pathways in PB allow facile accommodation and the release of the alkaline cations, thereby conferring PB an efficient color modulation material. However, moderate cyclic stability of PB film hinders its commercial development in EC devices because of its intrinsic structural imperfection and drastic volume expansion upon repeated charge-discharge cycling. Numerous research works have demonstrated some approaches to stabilize intrinsic PB structure through the electrodeposition of PB in the electrolytic bath with sufficient  $\text{K}^+$  ions [7] and cyclic process in KCl bath [8]. Apart from adjusting the electrodeposition parameters, suitable interfacial engineering on PB is also essential for cyclic stability. Considering polymer polyaniline (PANI) has shown its potential as a highly efficient and stable electrode in the supercapacitors [9,10], we attempt to integrate PANI with PB framework with the aim of improving the cyclic stability of the films as shown in Fig. 1. As confirmed by the microscopic images, the conventional cracking issues in PB films induced by the volume changes upon the drying process was reduced with the overlayer PANI, which ultimately enhances the cyclic stability of the PANI/PB system. By electrodepositing a layer of PB on ITO substrate, followed by subsequent PANI deposition, a stable electrode with high charge density ( $\sim 10 \text{ mC/cm}^2$ ) can be retained in KCl/DMSO chemical bath after the 60 charging/discharging cycles. The improvement in the electrochemical stability and morphological control were demonstrated based on

PANI/PB electrode by using cyclic voltammetry and microscopic images respectively.

## II. MATERIALS AND METHODS

### A. Preparation of the substrates:

The ITO-coated glass substrates were firstly cleaned with DI water, acetone and isopropanol in an ultrasonication bath for 25 minutes each. The ITO substrates were then blown dry with a nitrogen gun, followed by an oxygen plasma treatment for 15 minutes at RF power of 30 W and oxygen flow rate of 8 sccm.

### B. Electrodeposition of Prussian blue (PB) on ITO

Aqueous solution consisting of potassium ferricyanide III (10 mM), ferric chloride (10 mM), potassium chloride (50 mM) was prepared as an electrochemical bath. The pH of the solution was adjusted to 2 with the addition of hydrochloric acid. All chemicals were purchased from Sigma Aldrich and used as-received. Before the electrodeposition, the electrochemical bath was purged with pure nitrogen gas for 30 minutes to eliminate dissolved oxygen.

The electrodeposition process for PB growth was performed using a standard three-electrode configuration with ITO as working electrode, a Pt sheet as counter electrode and a Ag/AgCl electrode as reference electrode at room temperature. According to the profilometer measurement (Fig. 2), 260 nm thick PB films were electrodeposited under potentiostatic mode at 0.5 V (vs. Ag/AgCl) in the electrochemical bath for 500 seconds. Subsequent cleaning on PB surface was applied with DI water and ethanol to remove unreacted chemical residues, followed by drying in an oven at 60 °C for 2 hours.

### C. Electrodeposition of polyaniline on PB-coated ITO (PANI/PB):

Aqueous solution consisting of aniline (0.5 M) and sulfuric acid (1 M) was firstly mixed and purged under nitrogen gas for 30 minutes. 80 nm thick PANI film was electrodeposited under potentiostatic mode at 0.75 V (vs. Ag/AgCl) in the electrochemical bath for 90 seconds on PB-coated ITO (Fig. 2). Similar to the preparation process for PB films, subsequent cleaning and drying (60 °C for 2 hours) on PANI/PB surface was applied after the electrodeposition. The selection of deposition time was based on the adhesive strength of films on the ITO. For example, the aniline solution started to become green in color after electrodeposition time of 90 seconds, implying that the growth of polymer was no longer adhered on ITO but staying

in solution. As such, the deposition time for PANI on the ITO was set as 90 seconds.



Fig. 1. Schematic drawings of PANI/PB (left) and PB (right) films.

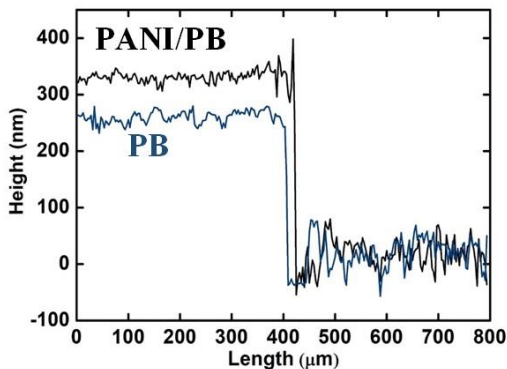


Fig. 2. Profilometer measurements on PANI/PB and PB films.

First, we should point out that electrodeposition is a low-cost scalable process to prepare uniform PB and PANI films on conducting substrates. As shown in Fig. 3, uniform thin films of bilayer PANI/PB and single PB layer can be grown on 25 mm x 25 mm sized ITO substrates. The intense blue color of the samples arose from the energy transfer of electrons from Fe(II) ions to Fe(III) ions inside the as-grown PB films [11].

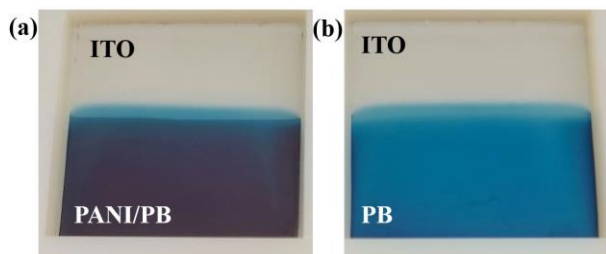


Fig. 3. Photographs of PANI/PB and PB films on ITO in colored state.

In this study, the drying temperature (60 °C for 2 hours) for the as-grown films were carefully selected in order to prevent triggering degradation of PANI upon thermal treatment [12]. Raman measurements were performed by WITec alpha300S Raman imaging systems under a laser source with wavelength of 532 nm in order to investigate any changes in the chemical states of PANI chains and PB after the drying process. According to the Raman spectra (Fig. 4), TABLE I and TABLE II, the signature Raman peaks of PANI and PB were observed in 60 °C dried sample along the band positions between 1220 – 1640  $\text{cm}^{-1}$  and 2090 – 2160  $\text{cm}^{-1}$ , confirming the formation of PANI [13] and PB [14] on ITO. However, the Raman energy bands for PANI was completely diminished when the drying temperature was increased from 60 °C to 80 °C, indicating

that the decomposition of PANI occurs at high temperature. Therefore, the conditions in drying all PB films were set as 60 °C for 2 hours.

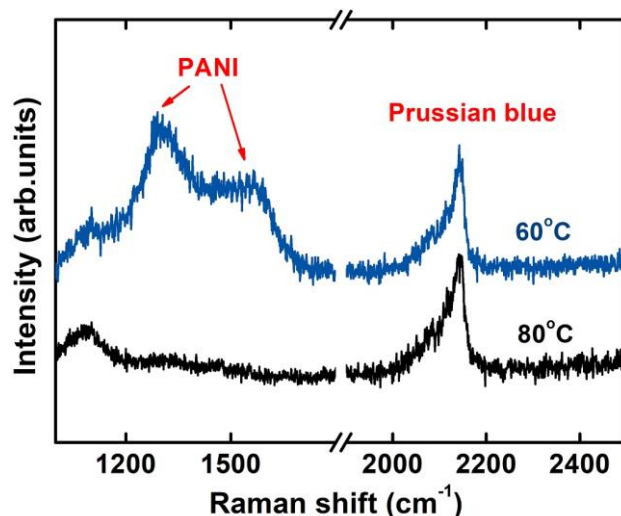


Fig. 4. Annealing effects on Raman characterization of PANI/PB films.

TABLE I. RAMAN BAND POSITION AND ASSIGNMENT OF PANI.

Band position ( $\text{cm}^{-1}$ )	Functional group/vibrations
1220	(C-N)
1250	C-N <sup>+</sup> def.
1340	(C-N <sup>+</sup> )
1470/1490	$\nu$ (C=N)
1560	$\nu$ (C-C) Q ring
1590	$\nu$ (C=C) Q ring
1620	$\nu$ (C-C) B ring
1640	$\nu$ (C-C) Pho, Phz

TABLE II. RAMAN BAND POSITION AND ASSIGNMENT OF PB.

Band position ( $\text{cm}^{-1}$ )	Functional group/vibrations
2090	$\nu$ (C≡N) of Fe <sup>II</sup> -CN-Fe <sup>III</sup>
2123	C-N <sup>+</sup>
2155-2160	$\nu$ (C≡N) of Fe <sup>II</sup> -CN-Fe <sup>III</sup>

PB film is a promising anodically coloring EC material, in which the film color can be modulated by oscillating between its oxidized state (colored Prussian blue) and reduced state (bleached Prussian white, PW) respectively [5]. As shown in Fig. 5a, high optical modulation in transmission ( $\Delta T$  is 63% @600nm) on PB film can be attained by applying a negative voltage of -1 V (vs. Ag/AgCl) for 20 s to transform colored PB into bleached PW or applying a positive voltage of +1 V (vs. Ag/AgCl) for 20 s to transform bleached PW into colored PB. Although PB film has good EC properties, the cracking issue on the PB surface remains an obstacle for commercial applications. Optical microscopic image taken on the electrodeposited PB surface (Fig. 6a) clearly shows the formation of micron-sized cracks on the dried PB film. Formation of cracks caused by material shrinkage upon

drying process is a common issue in electrodeposited PB thin film. As seen in Fig. 6b, after 10 cycles under continuous potential alternation between -1 V and +1 V (vs Ag/AgCl) for 20 s each in 0.027 M KCl/DMSO electrolyte, the PB film lost its adherence on ITO.

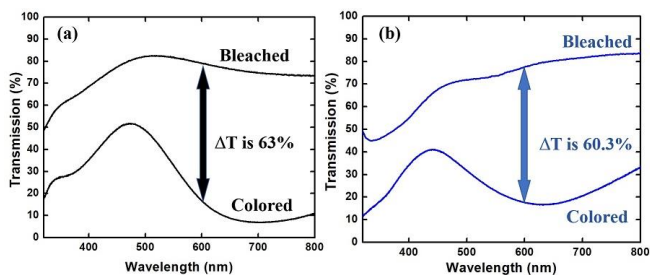


Fig. 5. Transmission spectra of (a) PB and (b) PANI/PB films under bleached state and colored state.

By contrast, PANI/PB film could demonstrate high EC optical modulation ( $\Delta T$  is 60.3% @600nm) (Fig. 5b) and good film adhesion to ITO simultaneously under repeated cycling (Fig. 7). Similar to PB film, PANI is also an anodically coloring EC material, which is optically complementary with PB at the optical modulation range (300-600 nm). PANI also acts as a protective overlayer to reduce the strain/material shrinkage induced inside the PB by the volume changes upon drying process and electrochemical cycling processes, which provides good electrochemical stability of the PANI/PB system.

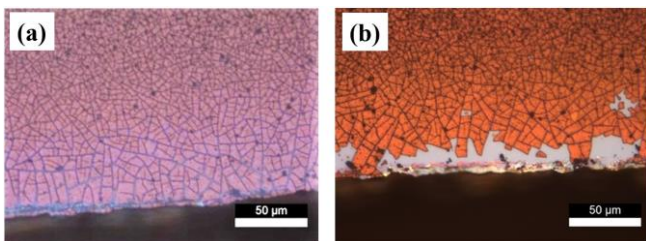


Fig. 6. Optical microscopic images of PB films taken (a) before and (b) after 10<sup>th</sup> cyclic test in KCl/DMSO electrolyte.

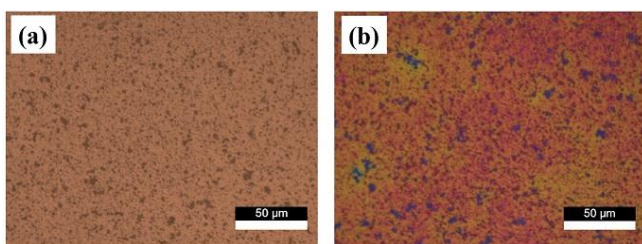


Fig. 7. Optical microscopic images of PANI/PB films taken (a) before and (b) after 10<sup>th</sup> cyclic test in KCl/DMSO electrolyte.

More stable charge-discharge behavior with higher current density (Fig. 8) can be attained from PANI/PB film than PB film upon sweeping between -1 V (bleaching) and +1 V (coloring). PANI overlayer could prevent the rapid dissolution/breaking of the cracked PB film under repeated cycling. As shown in Fig. 9, high charge density ( $\sim 10$  mC/cm<sup>2</sup>) with stable behavior (small loss of charge density, 8.74 % drop in the 60<sup>th</sup> cycle compared with the 1<sup>st</sup> cycle) was attained in PANI/PB film, while PB film has already lost 27.9 % in its charge density after 60 cycles.

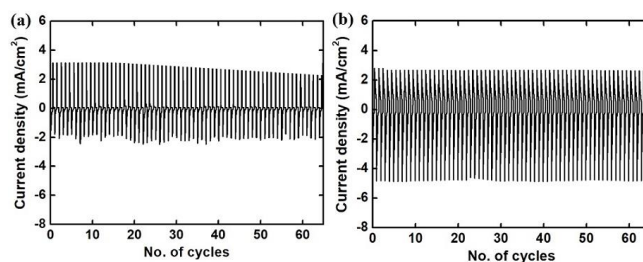


Fig. 8. Chronoamperometry of (a) PB and (b) PANI/PB films in KCl/DMSO electrolyte (-1 V, 20 s for bleaching/+1 V, 20 s for coloring).

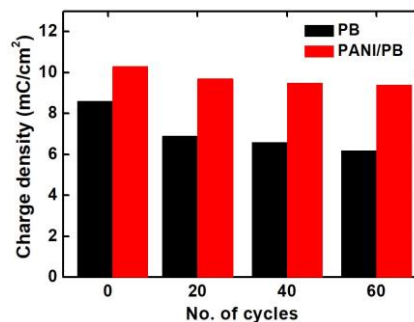


Fig. 9. Evaluation of the charge density of PB and PANI/PB films based on the integration of the current density over time measured at 1<sup>st</sup>, 20<sup>th</sup>, 40<sup>th</sup> and 60<sup>th</sup> cycles in Fig. 8.

To identify the charge storage kinetics of the PANI/PB and PB films, the current response at a particular potential along different scan rates ( $v$ ) in CV measurement was compared (Fig. 10). The CV spectra indicate that the charge storage kinetics are quasi-reversible processes since the peak potentials are a function of scan rate. Contrary to PB film, the sharper redox peaks with higher current corresponding to the processes of K<sup>+</sup> intercalation/deintercalation were observed in the CV response of PANI/PB film, suggesting that faster kinetic reactions happened with the aid of conductive PANI overlayer.

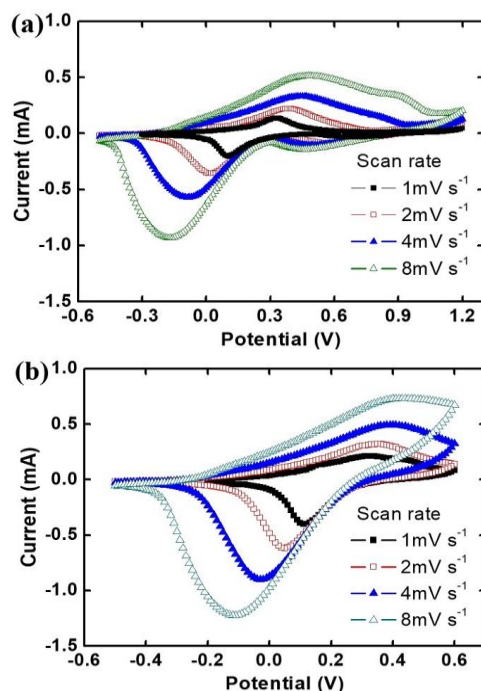


Fig. 10. CV plots of (a) PB and (b) PANI/PB films measured at different scan rates in KCl/DMSO electrolyte.

According to the power law, the scan rate-dependent CV response can be used to determine the  $b$  values based on the following equations [15,16]:

$$i_p = av^b \quad (1)$$

where  $i_p$  is peak current while  $a$  and  $b$  are adjustable values. Taking the logarithm of both sides in (1) gives

$$\log(i) = \log a + b \log(v) \quad (2)$$

The  $b$  values for PANI/PB and PB films can thus be extracted from the slopes of  $\log(i)$  versus  $\log(v)$  plots. For  $b$  values of 0.5 and 1, the charge storage mechanism is governed by diffusion-controlled reactions and surface-controlled capacitive behaviour respectively.

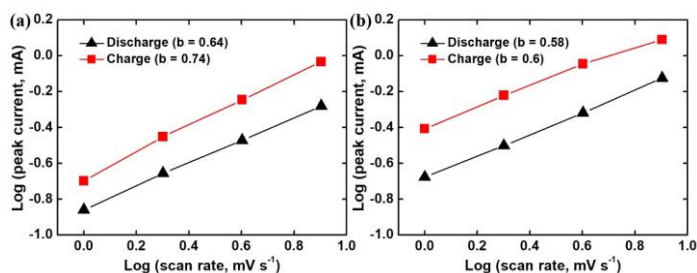


Fig. 11.  $b$  values from CV plots of (a) PB and (b) PANI/PB films.

Considering the  $b$  values are  $< 0.85$  (Fig. 11), the charges stored in both films are contributed by the diffusion-controlled reactions, rather than surface-controlled reactions, suggesting the charge storage mainly occurs at the inner surfaces of the films via the intercalation and deintercalation of  $K^+$  ions. It should be noted that the contribution of diffusion-controlled process in PANI/PB film ( $b$  is 0.6) is higher than that for PB film ( $b$  is 0.74) in KCl electrolyte, suggesting that the PANI overlayer could boost the  $K^+$  intercalation kinetics for better electrochemical performance.

#### IV. CONCLUSIONS

The electrodeposition of polyaniline/Prussian blue (PANI/PB) bilayer films displaying high electrochromic optical modulation and efficient diffusion-controlled charge storage kinetics was demonstrated. Due to the protective overlayer PANI, the strain induced inside the PB by the volume changes upon drying process was reduced to prevent cracking issue and thus displayed good electrochemical stability of the PANI/PB system. The low-cost scalable electrodeposition process, together with the good electrochemical behavior shows the potential of PANI/PB system for electrochemical applications.

#### ACKNOWLEDGMENT

This work was supported by the Institute of Materials Research and Engineering (IMRE) under the Agency for

Science, Technology, and Research (A\*STAR) via grant A19D9a0096 (SC25/19-8R1413-P1\_2) and Career Development Fund (C210112032). The authors would like to acknowledge the Raman measurement from Dr. Chen Mingxi.

#### REFERENCES

- [1] M. Qin, W. Ren, R. Jiang, Q. Li, X. Yao, S. Wang, Y. You, and L. Mai, "Highly crystallized Prussian blue with enhanced kinetics for highly efficient sodium storage", *ACS Appl. Mater. Interfaces*, vol. 13, pp. 3999–4007, January 2021.
- [2] J. Liu, W. Zhou, S. Walheim, Z. Wang, P. Lindemann, S. Heissler, J. Liu, P. G. Weidler, T. Schimmel, C. Wöll, and E. Redel "Electrochromic switching of monolithic Prussian blue thin film devices", *Optics Express*, vol. 23, pp. 13725–13733, May 2015.
- [3] C. Y. Jeong, T. Kubota, and K. Tajima, "Flexible electrochromic devices based on tungsten oxide and Prussian blue nanoparticles for automobile applications", *RSC Adv.*, vol. 11, pp. 28614–28620, August 2021.
- [4] R. Sanchis-Gual, T. F. Otero, M. Coronado-Puchau, and E. Coronado, "Enhancing the electrocatalytic activity and stability of Prussian blue analogues by increasing their electroactive sites through the introduction of Au nanoparticles" *Nanoscale*, vol. 13, pp. 12676–12686, June 2021.
- [5] H. Zhang, P. Li, S. Chen, F. Xie, and D. J. Riley, "Anodic transformation of a core-shell Prussian blue analogue to a bifunctional electrocatalyst for water splitting", *Adv. Funct. Mater.* vol. 31, pp. 2106835, November 2021.
- [6] S. W. Tong, W. P. Goh, X. Huang, and C. Jiang, "A review of transparent-reflective switchable glass technologies for building facades", *Renew. Sust. Energ. Rev.*, vol. 152, pp. 111615, December 2021.
- [7] M. Pyrasch and B. Tiede, "Electro- and photoresponsive films of Prussian blue prepared upon multiple sequential adsorption", *Langmuir*, vol. 17, pp. 7706–7709, November 2001.
- [8] V. B. Isfahani, H. R. Dizaji, N. Memarian, and A. Arab, "Electrodeposition of prussian blue films: study of deposition time effect on electrochemical properties", *Mater. Res. Express*, vol. 6, pp. 096449, July 2019.
- [9] S. S. Shah, H. T. Das, H. R. Barai, M. A. Aziz, "Boosting the Electrochemical Performance of Polyaniline by One-Step Electrochemical Deposition on Nickel Foam for High-Performance Asymmetric Supercapacitor", *Polymers*, vol. 14, pp. 270, January 2022.
- [10] S. S. Shah, M. A. Alfasane, I. A. Bakare, M. A. Aziz, Z. H. Yamani, "Polyaniline and heteroatoms-enriched carbon derived from *Pithophora polymorpha* composite for high performance supercapacitor", *J. Energy Storage.*, vol. 30, pp. 101562, August 2020.
- [11] V. Bayzi Isfahani, N. Memarian, Hamid Rezagholipour Dizaji, A. Arab, and M. M. Silva, "The physical and electrochromic properties of Prussian Blue thin films electrodeposited on ITO electrodes", *Electrochimica Acta*, vol. 304, pp. 282–291, May 2019.
- [12] S. A. Akbar, "Effect of drying temperature on polyaniline electrode for polyaniline/Zn battery performance", *Bull. Chem. Soc. Ethiop.*, vol. 33, pp. 551–559, 2019.
- [13] A. V. Syugaev, A. N. Maratkanova, A. A. Shakov, N. V. Lyalina, D. A. Smirnov, "Polyaniline films electrodeposited on iron from oxalic acid solution: spectroscopic analysis of chemical structure", *J Solid State Electrochem.*, vol. 22, pp. 3171–3182, June 2018.
- [14] G. Moretti, C. Gervais, "Raman spectroscopy of the photosensitive pigment Prussian blue", *J. Raman Spectrosc.*, vol. 49, pp. 1198–1204, February 2018.
- [15] T. Kim, W. Choi, H.-C. Shin, J.-Y. Choi, J. M. Kim, M.-S. Park, and W.-S. Yoon, "Applications of voltammetry in lithium ion battery research", *J. Electrochem. Sci. Technol.*, vol. 11, pp. 14–25, January 2020.
- [16] T. S. Mathis, N. Kurra, X. Wang, D. Pinto, P. Simon, and Y. Gogotsi, "Energy storage data reporting in perspective—guidelines for interpreting the performance of electrochemical energy storage systems", *Adv. Energy Mater.* vol. 9, pp. 1902007, September 2019.